Global Change Biology

Global Change Biology (2011) **17**, 3736–3746, doi: 10.1111/j.1365-2486.2011.02499.x

Quantifying the hydrological responses to climate change in an intact forested small watershed in Southern China

GUOYI ZHOU*, XIAOHUA WEI†, YIPING WU‡, SHUGUANG LIU§, YUHUI HUANG*, JUNHUA YAN*, DEQIANG ZHANG*, QIANMEI ZHANG*, JUXIU LIU*, ZE MENG*, CHUNLIN WANG¶, GUOWEI CHU*, SHIZHONG LIU*, XULI TANG* and XIAODONG LIU*

**South China Botanical Garden, Chinese Academy of Sciences, Guangzhou, 510650, China, †University of British Columbia (Okanagan), 3333 University Way, Kelowna British Columbia, V1V 1V7, Canada, ‡Arctic Slope Regional Corporation (ASRC) Research and Technology Solutions, Contractor to the U.S. Geological Survey (USGS) Earth Resources Observation and Science (EROS) Center, Sioux Falls, SD, 57198, USA, §U.S. Geological Survey (USGS) Earth Resources Observation and Science (EROS) Center, Sioux Falls, SD, 57198, USA, ¶Climate and Agrometeorology Center of Guangdong Province, China Meteorological Administration, Guangzhou, 510080, China*

Abstract

Responses of hydrological processes to climate change are key components in the Intergovernmental Panel for Climate Change (IPCC) assessment. Understanding these responses is critical for developing appropriate mitigation and adaptation strategies for sustainable water resources management and protection of public safety. However, these responses are not well understood and little long-term evidence exists. Herein, we show how climate change, specifically increased air temperature and storm intensity, can affect soil moisture dynamics and hydrological variables based on both long-term observation and model simulations using the Soil and Water Assessment Tool (SWAT) in an intact forested watershed (the Dinghushan Biosphere Reserve) in Southern China. Our results show that, although total annual precipitation changed little from 1950 to 2009, soil moisture decreased significantly. A significant decline was also found in the monthly 7-day low flow from 2000 to 2009. However, the maximum daily streamflow in the wet season and unconfined groundwater tables have significantly increased during the same 10-year period. The significant decreasing trends on soil moisture and low flow variables suggest that the study watershed is moving towards drought-like condition. Our analysis indicates that the intensification of rainfall storms and the increasing number of annual no-rain days were responsible for the increasing chance of both droughts and floods. We conclude that climate change has indeed induced more extreme hydrological events (e.g. droughts and floods) in this watershed and perhaps other areas of Southern China. This study also demonstrated usefulness of our research methodology and its possible applications on quantifying the impacts of climate change on hydrology in any other watersheds where long-term data are available and human disturbance is negligible.

Keywords: climate change, floods and droughts, intact watershed, long-term study, precipitation pattern, soil moisture

Received 23 April 2011 and accepted 7 June 2011

Introduction

Elevated atmospheric CO_2 concentration and climate change may have significant impacts on terrestrial hydrological cycle by altering the spatiotemporal distribution of precipitation, air temperature, evapotranspiration, plants, etc. (Saxe *et al*., 1998; Wand *et al*., 1999; Medlyn *et al*., 2001; Eckhardt & Ulbrich, 2003; Ficklin *et al*., 2009; Wu *et al*., 2011). Several large-scale studies based on modelling and observations implied that global climate change have altered the watershed hydrology (Easterling *et al*., 2000b; Jackson *et al*., 2001; Koster *et al*., 2004; Piao *et al*., 2009) and the intensification of rainfall storms is more notable than the change of annual amount in many areas of the world (Karl & Knight, 1998; Mason *et al*., 1999; Easterling *et al*., 2000a; New *et al*., 2001; Luo *et al*., 2008; Schiermeier, 2008; Piao *et al*., 2010; Qiu, 2010). For example, Piao *et al*. (2009, 2010) identified increased frequency of floods and droughts in China's cropland during the past 40 years as well as heat waves during the past 50 years.

In spite of growing interest in assessing the impacts of climate change on hydrology, few studies have dealt with the underlying mechanism of hydrological responses to climate change (IPCC, 2007; Schiermeier, 2008; Qiu, 2010). Due to interactive effect of climate change and land use shifts, it is challenging to quantify the relative contribution of climate change to hydrology without removing the effect of land use changes (Shukla & Mintz, 1982; Koster & Suarez, 2003; Qiu, 2010; Wei & Zhang, 2010b; Zhou *et al*., 2010). The lack

Correspondence: Guoyi Zhou, tel. +86 20 3725 2708, fax +86 20 3725 2615, e-mail: gyzhou@scib.ac.cn

of a suitable and commonly accepted research methodology may be the major reason for this challenge (Wei & Zhang, 2010a). Statistical and hydrological models are frequently used to assess climate change effect on hydrology but each approach has its own weakness (Wei & Zhang, 2010a; Zhang *et al.*, 2011). Where data are appropriate and long-term, and statistical assumptions are met, statistical techniques or models are useful to develop inference between hydrological parameters and responsible variables. Statistical models do not provide information on the underlying physical processes that control hydrological response. Physically based hydrological models, such as DHSVM, MIKE-SHE and VIC require time-consuming calibration and validation process, as well as large datasets including topography, vegetation, climate and hydrology. In particular, hydrological models need empirical data and relationships to validate the interactive effect of climate and land use changes on hydrology (if their relative contributions must be separated), which are normally not available. Therefore, alternative methods must be explored to quantify the hydrological effects of climate change.

Globally, soil moisture is not monitored as regularly as temperature or precipitation because it is not easily collected (Robock & Li, 2006; Schiermeier, 2008). Clarifying the relationship between climate change and soil moisture is difficult because there are few continuous soil moisture monitoring sites around the world (Robock & Li, 2006; Schiermeier, 2008; Piao *et al.*, 2009). Although numerous modelling studies discussed the change between soil moisture and air temperature as well as rainfall (Hong & Kalnay, 2000; Seneviratne *et al.*, 2006; Fischer *et al.*, 2007), climate change and soil moisture relationships are not well understood due to limited data (Dirmeyer, 2000; Koster *et al.*, 2004; Schiermeier, 2008). Further, the substantial uncertainty of climate projections using General Circulation Models (GCMs) (Wolock & McCabe, 1999) also hinders scientific progresses in assessing regional climate change impacts on ecosystems and water resources (Milly *et al.*, 2008; Schiermeier, 2008).

In this study, to quantify the impacts of climate change on soil moisture and hydrology in Southern China, we used a unique design of a long-term monitoring programme and hydrological modelling with Soil and Water Assessment Tool (SWAT) in an intact forested watershed. The intact forested watershed (Dinghushan Bioshere Reserve or DBR) is dominated by regional climax evergreen broadleaved forest, which has not been disturbed in the last 60 years. Selection of this watershed allows removal of the confounding effect of land use change so that the effects of climate change can be effectively quantified. Long-term observations including precipitation, air temperature, soil moisture, streamflow and groundwater table, etc. can help us to understand the occurred climate change and hydrological processes, while SWAT model can be used to investigate the processes and mechanisms as to how climate change affect hydrological processes. The combination of long-term data with a hydrological model offers better and complementary opportunity to assess the impacts of climate change on soil moisture and hydrology.

Materials and methods

Study area

Dinghushan Bioshere Reserve (23°09′21″N–23°11′30″N, 112°32′39″E–112°35′41″E) is located about 84 km west of Guangzhou in central Guangdong province, Southern China (Fig. 1). It was established in 1950 to protect natural monsoon evergreen broadleaved forests (MBF) in the lower subtropics and was accredited as the first National Natural Reserve in China in 1956. The reserve covers an area of 1156 ha, divided into eastern and western watersheds of area 613.2 ha and 542.8 ha, respectively. The elevation ranges from 14 to 1000 m above sea level. The region has a typical southern subtropical monsoon climate, with annual average precipitation of 1678 mm, of which nearly 80% falls in the wet season (April–September) and the other 20% falls in the dry season (October–March). The annual mean temperature and relative humidity are 22.3 °C and 77.7%, respectively. The bedrock is sandstone and shale. Soils have a pH 4.0–4.9 and are classified in the ultisol group and udult subgroup according to USDA soil classification system (Buol *et al.*, 2003).

There were no changes in land covers and uses in DBR before and after 1950s. In addition to the MBF, pine forests (PF) and mixed pine and broadleaved forests (PBF) are other two most common forest communities that represent the early- and mid-successional stages of MBF, respectively. The age of the youngest forest type (PF) is older than 60 years. Previous studies in the study area showed that, although the total biomass of several succession vegetation types has been increasing, their leaf biomass has kept relative constant with an insignificant downtrend since 1980s (Zhou *et al.*, 2007; Tang *et al.*, 2011), and no yearly uptrend in transpiration was found (Yan *et al.*, 2001a,b).

All the long-term observations on soil moisture, stream discharge and groundwater tables were conducted in the eastern watershed of DBR (Fig. 1). The rationale for selecting sites to monitor streamflow, groundwater level and soil moisture was to assess dynamic responses of those hydrological variables to climate variability and construct water budget in an intact, forested watershed. Therefore, the distribution of the probes installed in 1979 was based on the two factors: representation of spatial watershed soil moisture as much as possible and easy deployment of equipment. Soil moisture monitoring sites were located in six major forested catchments of the eastern watershed, two for MBF, three for PBF and one for PF. The

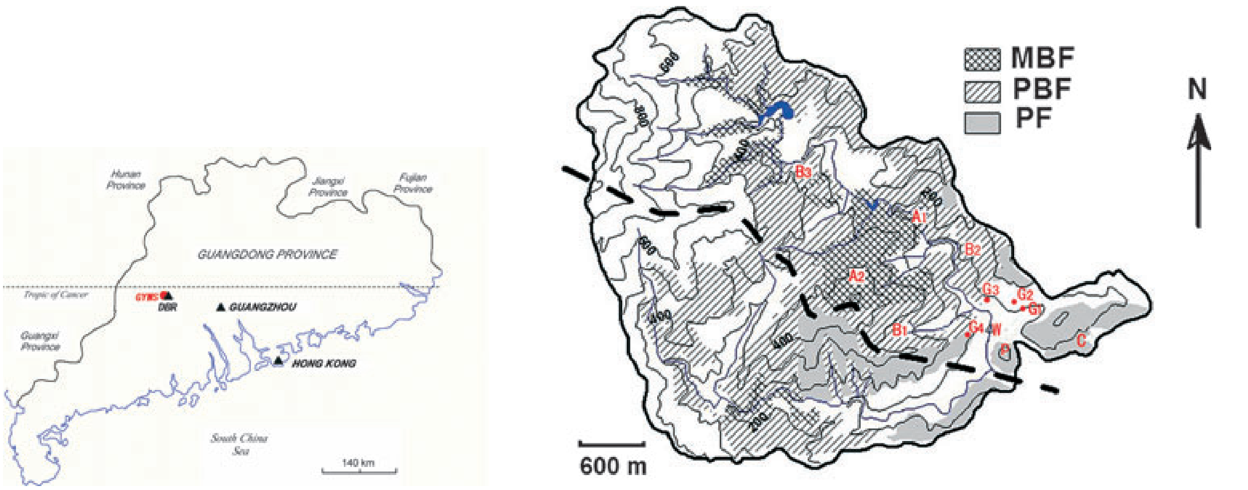

Fig. 1 Locations (left panel) of Dinghushan Biosphere Reserve (DBR) (black solid triangle) and Gaoyao Weather Station (GYWS) (red solid circle) and topographical map (right panel) of DBR. DBR is divided into eastern (upper and right) and western (lower and left) watersheds and covered with three major vegetation communities. A (1-2)-MBF (monsoon evergreen broadleaved forest), B (1–3)-PBF (mixed pine and broadleaved forests), C-PF (pine forest), G(1–4)-groundwater wells, P-weather station and W-hydrological station.

areas of the six catchments range from 4 to 30 ha. Stream discharge and groundwater tables were measured through hydrological weir and four groundwater wells, respectively, that were located near the outlet of the watershed. The four groundwater wells were used to monitor the groundwater table dynamics of the unconfined aquifer in the downstream of DBR. These wells are located in the range of 60–150 m from the weir, and their elevations are 2–6 m higher than the weir.

Soil moisture

Soil moistures were measured using both neutron probe and gravimetric sampling since 1979 (Table 1) in six forested catchments (A1, A2, B1, B2, B3, C as shown in Fig. 1) of the eastern watershed. Nine neutron probes were installed in each catchment, evenly arranged in upper, middle and lower parts of each catchment. Therefore, there are a total of 54 neutron probes. In the top 90 cm soil layer, six layers (0–15 cm, 15–30 cm, 30–45 cm, 45–60 cm, 60–75 cm and 75–90 cm) were subdivided. Three to six measurements (usually every 5 days) were made monthly using neutron probe method. Next to the neutron probes, soil samples were collected monthly with a 30 mm diameter auger to determine the gravimetric soil moisture contents corresponding to the same layers as sampled by neutron probe method. All results were changed into volumetric water content (%) of respective soil layers after being combined with soil bulk density.

Soil water characteristic curve (SWCC)

The SWCC was determined in three forested catchments, A1, B2 and C, in 2006. Three measurement locations were selected and evenly arranged in upper, middle and lower parts of each catchment, which are close to neutron probes. Therefore, there are nine SWCC measurement locations in total. Five sampling points at each measurement location were randomly selected. Soil cores in each of the nine layers (0–10 cm, 10–20 cm, 20–30 cm, 30–40 cm, 40–50 cm, 50–60 cm, 60–70 cm, 70–80 cm and 80–90 cm) were taken using stainless steel corer (5.65 cm in diameter, 4 cm in depth and 100 cm^3 in volume). Soil moisture was measured gravimetrically and soil water potential (Table 1) was determined using centrifugation (Hassler & Brunner, 1945).

Streamflow and groundwater table

The daily streamflow data were collected at the hydrological station (marked with 'W' in Fig. 1) which controls the eastern watershed. Streamflow was recorded automatically with both digital (WGZ-1, resolution ≤1 mm) and mechanical

Table 1 Measurement description of a number of variables

No.	Variable	Measurement method	Measurement period
1	Soil moisture	Neutron probe and gravimetric sampling	1979–2009*
2	Soil water potential	Centrifugation	2006
3	Groundwater table	Groundwater well	1999–2009
4	Streamflow	Hydraulic weir	2000–2009
5	Daily precipitation and air temperature	Gaoyao weather station	1954–2009

Note: *With missing values in some years.

equipments (HCJ1, resolution ≤1 mm) at the weir. Within the range of 150 m from the hydrological weir, there are four groundwater wells (marked G1, G2, G3 and G4 in Fig. 1) used to manually measure groundwater tables once every 5 days. The groundwater table was directly determined by manually measuring the depth below land surface with a floating device.

Precipitation and air temperature

Daily air temperature and precipitation representing the DBR's climatic regime were obtained from the Gaoyao Weather Station, 10 km from DBR. There are no significant differences in air temperature and precipitation between the Gaoyao Weather Station and DBR Weather Station (Yan *et al.*, 2003) (Fig. 1).

Statistical analysis

Prior to any statistical analysis, data must be checked on normality, autocorrelation etc. Where data do not meet those statistical assumptions, data were transferred or alternative statistical tests (i.e. distribution-free non-parametric test) were applied. We used the least squares method to obtain the linear fits of trends in air temperature, precipitation, soil moistures, groundwater tables, annual ratio of water yield to precipitation, monthly 7-day low flow and the maximum daily flow in May and June (Figs 2 and 3). If the slopes of fitted linear lines are significantly different from zero (t-test: $P < 0.05$), the trends are considered to be statistically significant.

SWAT and its modification

The SWAT model was developed by the USDA Agricultural Research Service (Arnold *et al.*, 1998) for exploring the effects of climate and land management practices on water, sediment and agricultural chemical yields. This physically based watershed scale model simulates the hydrological cycle, cycles of plant growth, the transportation of sediment and agricultural chemical yields on a daily time step (Arnold *et al.*, 1998; Neitsch *et al.*, 2005). The hydrological part of the model is based on the water balance equation in the soil profile with processes, including precipitation, surface runoff, infiltration, evapotranspiration, lateral flow, percolation and groundwater flow (Arnold *et al.*, 1998; Neitsch *et al.*, 2005).

For simulating baseflow in SWAT, $Q_{b,i}$, on a given day i (mm/day), the following equation was adopted (Neitsch *et al.*, 2005),

$$Q_{b,i} = Q_{b,i-1} \cdot e^{-\alpha_b \cdot \Delta t} + W_{rchg,i} \cdot (1 - e^{-\alpha_b \cdot \Delta t}) \tag{1}$$

where α_b is the baseflow recession constant, Δt is the time step (1 day), and $W_{rchg,i}$ is the amount of recharge entering the aquifer on day i (mm day^{-1}), and is calculated by the equation below,

$$W_{rchg,i} = W_{seep} \cdot (1 - e^{-1/\delta_b}) + W_{rchg,i-1} \cdot e^{-1/\delta_b} \tag{2}$$

where δ_b is the delay time or drainage time of the overlying geological formation (days), W_{seep} is the total amount of water

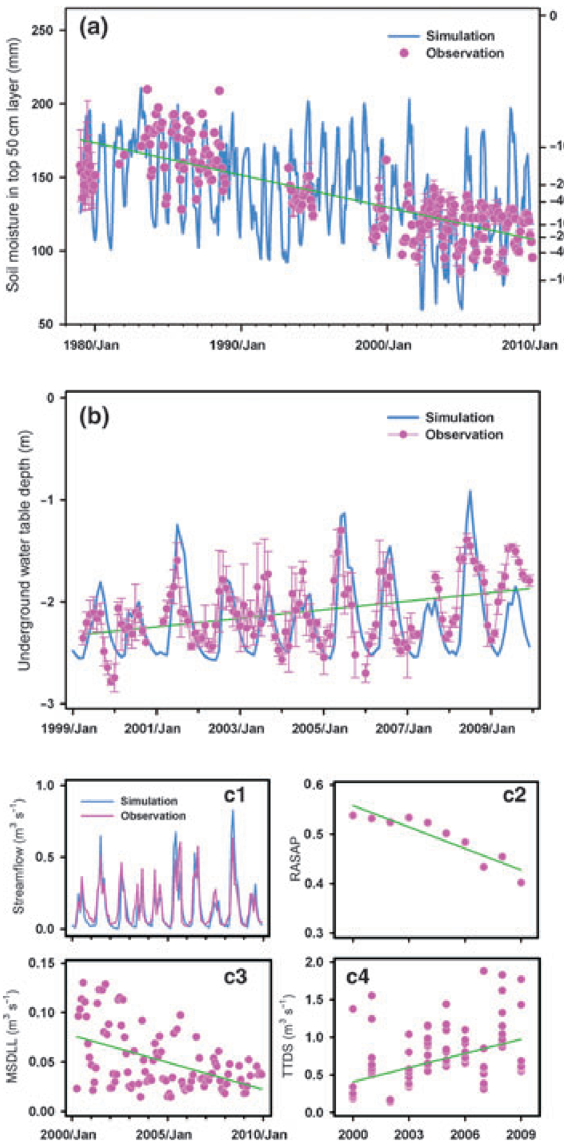

Fig. 2 Temporal trends in soil moisture, groundwater table and streamflow in Dinghushan Biosphere Reserve (DBR), with error bars as standard deviations; (a) monthly soil moisture during 1979–2009 and the corresponding soil water potential in the top 50 cm soil layer ($y = -2.2x + 4502.2$, $R^2 = 0.63$, $n = 218$, $P < 0.0001$, y-soil moisture (mm); x-year); (b) monthly groundwater table near the outlet during 1999–2009 ($y = 0.042x - 86.3$, $R^2 = 0.17$, $n = 119$, $P < 0.0001$, y-groundwater table (m), x-year); (c) monthly hydrograph and other characteristics of streamflow in the outlet during 2000–2009; c1-monthly hydrograph; c2-ratio of dry season streamflow to the precipitation (RASAP) ($y = -0.015x + 29.6$, $R^2 = 0.84$, $n = 10$, $P = 0.0001$, y-RASAP, x-year); c3-monthly 7-day low flow (MSDLL) in each month ($y = -0.0058x + 11.6$, $R^2 = 0.27$, $n = 120$, $P < 0.0001$, y-MSDLL (m^3 s^{-1}), x-year); and c4-the top ten daily stremflow (TTDS) in May and June ($y = -0.063x - 125.4$, $R^2 = 0.20$, $n = 100$, $P < 0.0001$, y-TTDS (m^3 s^{-1}), x-year).

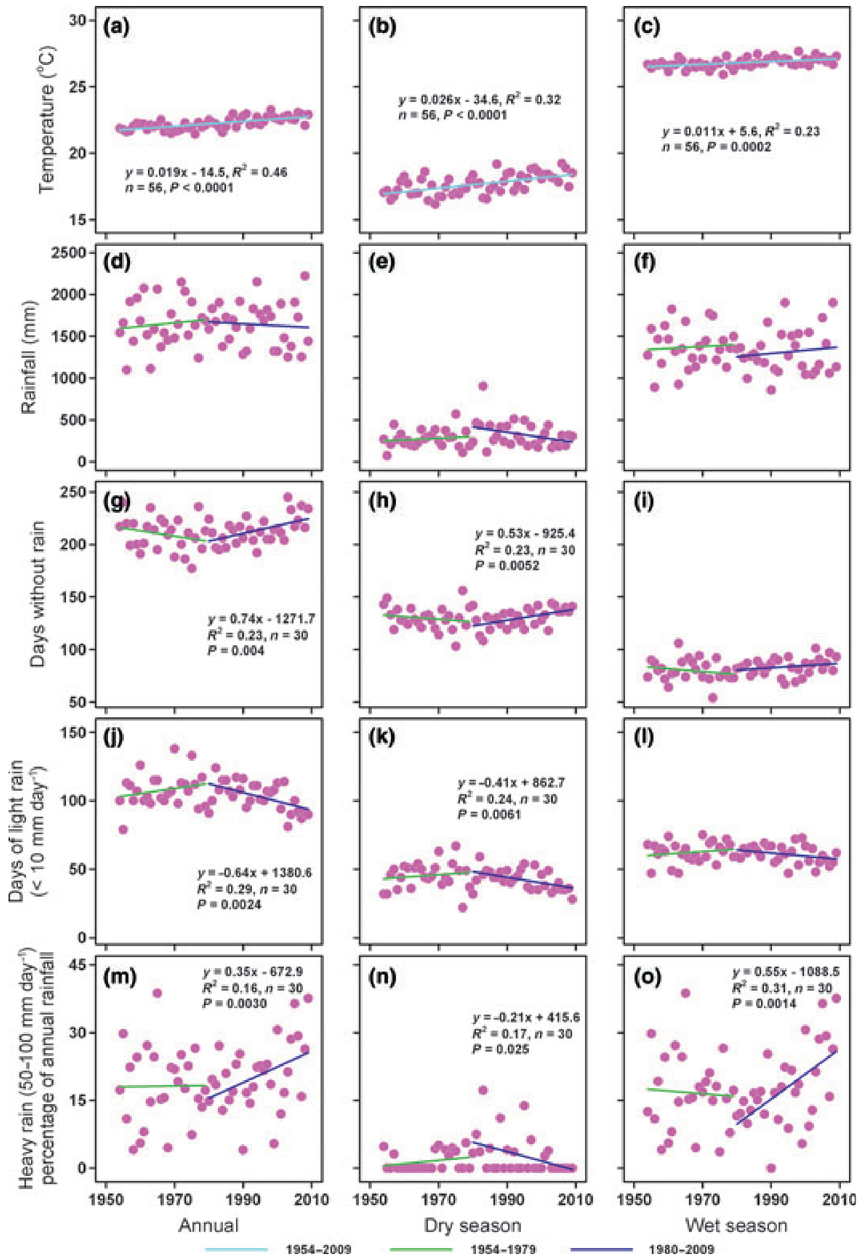

Fig. 3 Trends in annual periods, dry seasons and wet seasons of mean air temperatures (a, b, c), total rainfall (d, e, f), total no-rain days (g, h, i), total light-rain days (with precipitation intensities less than 10 mm day^{-1}) (j, k, l) and the percentage of annual rainfall in the intensity range of 50–100 mm day^{-1} to the annual total (APARI) (m, n, o) during 1954–2009, 1954–1979 and 1980–2009. Significant ($P < 0.05$) trends for both periods of 1954–2009 and 1954–1979 were found only for air temperature. The trends with statistic significance ($P < 0.05$) in the period of 1980–2009 are depicted with regression equations in the respective panels.

exiting the bottom of the soil profile on day i (mm day^{-1}), and $W_{rchg,i-1}$ is the amount of recharge entering aquifer on day i-1 (mm day^{-1}).

According to Neitsch *et al.* (2005), the calculation of baseflow in SWAT is a function of seepage from the soil profile in addition to two parameters, delay time of recharge δ_b and baseflow recession constant α_b, which determine how fast the seepage enters the groundwater system and how fast the water in the shallow aquifer discharges to a river or lake, respectively. However, we found this baseflow representation is not suitable for our study area, because the simulated groundwater table (i.e. shallow aquifer water content) cannot match well with the observations, no matter how we calibrate the above two parameters under the premise of satisfactory simulation of soil moisture and streamflow. Therefore, we proposed an alternative equation to represent the baseflow process in the study area as shown below,

$$Q_{b,i} = a \times \left(\frac{W_{gw,i} - GWQMN}{W_{gw,mx} - GWQMN} \right)^b \quad (3)$$

where $Q_{b,i}$ is the baseflow on a given day i (mm/day), $W_{gw,i}$ is the water in the shallow aquifer on a given day i (mm), $GWQMN$ is the threshold depth of water in the shallow aquifer required for baseflow to occur (mm), which is an existing parameter in SWAT, $W_{gw,mx}$ is the maximum allowable depth of water in the shallow aquifer (mm), a and b are linear and exponential coefficients to be calibrated.

Once baseflow, $Q_{b,i}$ is obtained by the above equation at a daily time step, it is updated considering the memory effect of groundwater flow using the following equation,

$$Q_{b,i}' = Q_{b,i-1}' \cdot e^{-\alpha_b \cdot \Delta t} + Q_{b,i} \cdot (1 - e^{-\alpha_b \cdot \Delta t}) \quad (4)$$

where $Q_{b,i}'$ is the updated baseflow on a given day i (mm/day), $Q_{b,i\text{-}1}'$ is the baseflow calculated on a previous day i-1 (mm day^1), Δt is the time step (1 day), and α_b is the baseflow recession constant.

Thus, the original SWAT was modified by incorporating the above new method for baseflow simulation. Comparing to the original method, adoption of the new method in SWAT involved two existing parameters (i.e. α_b, and $GWQMN$) and three extra parameters (i.e. a, b, and $W_{gw,mx}$). Since $GWQMN$ and $W_{gw,mx}$ can be estimated as the minimum and maximum observed amounts of water in the shallow aquifer (i.e. corresponding to the lowest and highest observed groundwater tables), three parameters, a, b and α_b need to be calibrated for baseflow simulation.

Model input

The SWAT model requires inputs on weather, topography, soils, land cover and land management (Arnold *et al.*, 2000). In this study, a Geographic Information System (GIS) interface, ArcSWAT (Winchell *et al.*, 2009) was used to automate the development of input parameters for SWAT. The 10-m digital elevation model (DEM) data for delineating sub-basins and this discretization resulted in the definition of 78 subbasins for the DBR. The land cover and soil data from field survey and *Guangdong Soil* (Guangdong Soil Survey Office (GSSO), 1993 were used to parameterize the SWAT model. The multiple Hydrological Response Unit (HRU) model option was used for representing the dominant land uses and soil types as separate HRUs within a subbasin. As a result, the study area was divided into 136 HRUs. Considering the small size of our study area and the major type of land cover (MBF, PBF and PF), the delineation of subbasins and HRUs can represent the DBR landscape for hydrological modelling.

Model calibration and validation

Through investigation of literature related to SWAT calibration (Santhi *et al.*, 2001; Muleta & Nicklow, 2005; Arabi *et al.*, 2008) as well as testing of sensitive parameters reported therein, eight parameters involved in the original SWAT were selected for model calibration. By including the three extra parameters (i.e. a, b and $W_{gw,mx}$, see Section Streamflow and groundwater table) when using the new method to estimate baseflow, a total of eleven parameters were finally selected (Table 2).

Although the observation for soil moisture could cover a longer time (from 1979 to 2009 with missing values for some years), groundwater table and streamflow were only measured for 10 years from 2000 to 2009. As a result, the SWAT model was calibrated and validated using 6-year (2000–2005) and 4-year (2006–2009) observation data, respectively, including streamflow, groundwater table and soil moisture. The SWAT built-in auto-calibration procedure (van Griensven *et al.*, 2006; Green & van Griensven, 2008), which is for streamflow and other constituents in the channel, is modified

Table 2 Calibrated parameters for the eastern watershed of Dinghushan Biosphere Reserve (DBR)

Parameter	Description	Range	Calibrated value/change
CN2	SCS curve number for moisture condition II	−8 to +8%	−4%*
ESCO	Soil evaporation compensation factor	0.001–1	0.75
EPCO	Plant uptake compensation factor	0.001–1	0.6
SOL_AWC	Soil available water capacity (mm H_2O/mm Soil)	0–1	0.23
SOL_K	Saturated hydraulic conductivity (mm h^{-1})	0–100	12
GW_delay	Groundwater delay (days)	0–31	4
GWQMN	Threshold depth of water in the shallow aquifer required for baseflow to occur (mm)	0–500	300‡
ALPHA_BF	Baseflow alpha factor (days)	0–1	0.5
$W_{gw,mx}$	Maximum amount of water in the shallow aquifer (mm)	–	450†
a	Linear parameter for baseflow estimation	0–1	0.015
b	Exponential parameter for baseflow estimation	0–1	0.04

Note: *Means relative changes of parameters to their default values,
‡Means it is taken from the minimum observed water amount in the shallow aquifer instead of trial-and-error,
†Means it is taken from the maximum observed water amount in the shallow aquifer instead of trial-and-error.

for the three variables of interest (streamflow, soil moisture and groundwater table) in our study.

Modelling of intensified rainfall and increased temperature

To assess the connections between climate change and hydrological variables, the calibrated SWAT model was applied to compare the following three different scenarios: Reference Scenario is the one with low intensity rainfall of 1975, Scenario 1 refers to high intensity rainfall of 2005 and air temperature of 1975, and Scenario 2 refers to high intensity rainfall of 2005 and high temperature of 2005. Total annual precipitations in 1975 and 2005 are the same, but rainfall intensities are different. All other variables remain the same for comparison purpose among the three scenarios. This comparison with a physically based model can help to investigate the impacts of changed rainfall and temperature on specific hydrological processes (surface runoff, soil moisture, groundwater level) when measurements cannot be easily implemented.

Results and discussion

Model evaluation

As mentioned previously, the SWAT model was calibrated and validated using 6-year and 4-year observation data, respectively, including streamflow, groundwater table and soil moisture. The calibrated values of these parameters are listed in Table 2. The model performance given in Table 3 indicates that the SWAT model is satisfactory ($P < 0.00001$) in simulating monthly streamflow with R^2 being 0.78 and 0.66 for calibration and validation, respectively. However, the R^2 values for simulating groundwater table and soil moisture were as low as 0.4 and 0.24, respectively, for the validation period. This may be due to relatively large spatial variations on those two parameters, as compared to SWAT simulated values. Nevertheless, the visual comparison shows a good fit between the observations and simulated values, particularly for the patterns and trends (i.e. decreasing soil moisture and rising groundwater table) (Fig. 2).

Table 3 Evaluation of model performance in simulating streamflow, groundwater table, and soil moisture during the calibration (2000–2005) and validation (2006–2009) periods

Variable	Period	PE (%)	R^2
Streamflow	Calibration	−13.67	0.66
	Validation	4.74	0.78
GW table	Calibration	1.42	0.33
	Validation	8.61	0.40
Soil moisture	Calibration	11.12	0.39
	Validation	16.90	0.24

Note: PE, percent error (Green & van Griensven, 2008).

Trends in air temperature and precipitation

In the past five decades, the annual temperature and temperatures in both dry (October–March next year) and wet (April–September) seasons in the DBR region increased significantly by approximately 1.0 ± 0.1 °C, 1.3 ± 0.6 °C and 0.6 ± 0.2 °C (Fig. 3a-c), respectively. The total amount of rainfall over the annual period, dry seasons and wet seasons did not show any significant changes (Fig. 3d-f). However, the annual number of no-rain days has significantly increased (Fig. 3g) and the annual number of light-rain days (i.e. with rainfall <10 mm day^{-1}) has decreased significantly (Fig. 3j) since 1980. The increase in no-rain days and decrease in light-rain days were statistically significant in the dry season (Fig. 3h and k), but not significant ($P > 0.05$) in the wet season (Fig. 3i and l). The annual proportional amount of rainfall with intensity (APARI) of 50–100 mm day^{-1} has significantly increased since around 1980 (Fig. 3m). The annual increasing trend in APARI can be mainly caused by the significant increase in APARI in wet season (Fig. 3o) even though the decreasing trend APARI in dry season is also statistically significant (Fig. 3n). In short, the air temperature has been increasing, while total rainfall shows no significant change since 1954 in the DBR region. However, rainfall patterns have been shifted towards more severe storms in the wet seasons, and more no-rain days and less light-rain days in dry season since around 1980.

Trends in hydrological variables

A significant declining trend in soil moisture starting from the early 1980s is apparent in Fig. 2a. Based on the observation data, the mean rates of decrease were −2.2 ± 0.1 mm yr^{-1} and this trend was different from zero at $\alpha = 0.05$ (*t*-test). The mean dry season (October–March) soil moisture decreased from 162.3 mm in 1983 to 107.4 mm in 2009. The soil moisture in the wet season (April–September) decreased from 186.6 mm in 1983 to 122.5 mm in 2009 and the soil water potential decreased from about −15 kPa in the early 1980s to about −200 kPa in 2009. In natural broadleaved forests, trees are stressed when soil water potential falls below −100 kPa in humid Southern China (Gao *et al.*, 2002). Considering the dynamic soil water potential, tree growth in DBR could have been started since 1980s, especially after 2001.

Soil water potential values were about −15 to −50 kPa year round (Fig. 2a) from 1979 to the early 1980s and this may indicate that the forest soils in DBR were rather wet (close to the soil field capacity in the wet season). Only since around 1980 when precipitation regime has significantly changed and air temperature has been increasing, did the soil moistures show a declining trend. The soil moisture declines coincided with the change in rainfall patterns that are characterized as more no-rain days and more intensified storms as described previously.

Data on groundwater tables measured in the lower reach of the watershed showed a significantly ($P < 0.0001$) increasing trend since the starting of observation in 1999 (Fig. 2b). The mean rates of increase were 4.2 ± 0.9 cm yr^{-1}. The trend was different from zero at $\alpha = 0.05$ (t-test).

Although no apparent trend ($P > 0.05$) in monthly streamflow has been detected for the past decade since the observation began (Fig. 2c1), both the ratios of dry season streamflow to the precipitation (RASAP, water yield coefficient) (Fig. 2c2) and monthly 7-day low flows (MSDLL) (Fig. 2c3) have been significantly decreasing ($P < 0.0001$). On the contrary, the high daily streamflow values (the 1st to 10th ranks) in May and June (TTDS) show a significant increase trend ($P < 0.0001$) (Fig. 2c4).

Overall, decline in soil moisture, water yield coefficient and monthly 7-day low flow demonstrate an uptrend in drought, and rising in high flows and groundwater tables suggest an increasing risk in flooding events. Clearly, climate change has pushed hydrological regime to two opposite extremes by increasing chance of both floods and droughts as a result of change in rainfall intensity and air temperature.

Simulated hydrological impacts of changed climate

Changed climate in the DBR was characterized by the intensified rainfall and increased temperature and its effects on hydrological variables were assessed using the calibrated SWAT model. Both Table 4 and Fig. 4 present the simulation results under the three different scenarios stated previously. Figure 4a shows that soil moisture decreased significantly especially in the dry season due to the elongation of no-rain days, and consequently led to the reduction of actual evapotranspiration (ET) (Table 4; Fig. 4b) in the dry season even if the potential evapotranspiration (PET) remained unchanged (Scenario 1: high intensity rainfall and low temperature in 1975). The increased PET due to the higher temperature can slightly raise the actual ET due to the insufficient soil moisture in the dry season and this temperature effect was much less than that of the changed rainfall pattern. Therefore, the changed rainfall pattern was the dominating factor, which led to decreases of about 10% in soil moisture and 19% in annual average ET (Table 4). From Fig. 4c and d, the intensified rainfall raised the annual groundwater table by 5.8% and increased the surface runoff by 143% in the wet season. Figure 4e shows that the peak streamflow in 2005 was much larger than that in 1975 during April to July when soil moistures were at rela-

Table 4 Comparisons of hydrological responses to three different climate change scenarios

	Observation/simulation			Relative change†	
	Reference	Scenario 1	Scenario 2	Scenario 1	Scenario 2
	Low intensity P	High intensity P and low T	High intensity P and high T	High intensity P and low T	High intensity P and high T
Year	1975	2005		–	–
P (mm)*	1909	1905	Nearly no change		
Number of dry days*	177	217		22.6%	
Air temperature (°C)*	21.90	21.90	22.53	–	0.63
PET (mm)	1165	1165	1182	–	1.5%
ET (mm)	941	758	765	−19.4%	−18.7%
Water in the 50 cm soil (mm)	149	134	134	−10.1%	−10.1%
Surface runoff (mm)	56	136	137	143%	143%
Lateral flow (mm)	351	403	413	14.8%	17.7%
Baseflow (mm)	528	632	616	19.7%	16.7%
Water yield (mm)	935	1171	1165	25.2%	24.6%
Groundwater recharge (mm)	579	664	650	14.7%	12.3%
GW table depth (m)	−2.08	−1.96	−1.96	5.8%	5.8%

Note: †The changes of the two scenarios relative to the reference;
*Observed data; P, precipitation; T, air temperature; PET, potential evapotranspiration; ET, actual evapotranspiration; and GW, Groundwater.

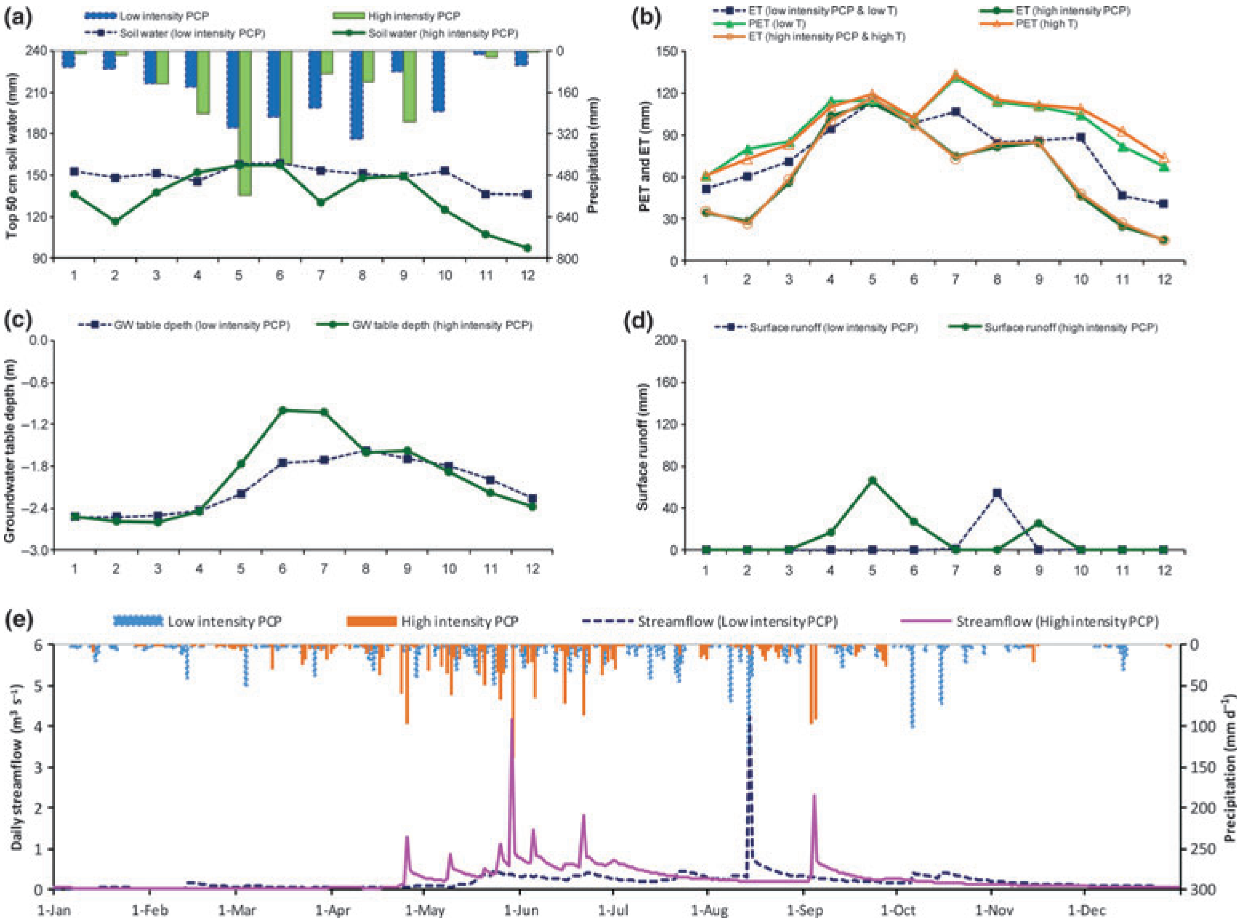

Fig. 4 Simulated responses of some hydrological parameters to intensified rainfall and increased air temperature in the DBR region under the low intensity rainfall (1975) and the high intensity rainfall (2005) (the total amounts of rainfall in 1975 and 2005 were nearly the same, 1909 and 1905 mm, respectively; P is precipitation, T is temperature, and GW is groundwater); and (a) monthly soil moisture content in the top 50 cm soil layer; (b) monthly PET and ET; (c) monthly groundwater (shallow aquifer) table depth; (d) monthly surface runoff; (e) daily streamflow.

tively high levels, with 113% of increase in streamflow under an increasing of 45% in rainfall during the 4-month period. In contrast, about 42% of decrease in streamflow during the other eight months (i.e. August–March) in 2005 was estimated when rainfall declined by 31% during this period. The annual water yield under the high intensity rainfall was raised by 25% compared to that under the low intensity rainfall (Table 4). Clearly, the changed rainfall pattern exacerbated both droughts and floods in the annual scale.

Implications

The simulations demonstrated that the observed soil drying, high streamflow increasing, and elevated groundwater tables were controlled by the change in precipitation patterns and air temperature. The intensified rainfall did not raise the soil moisture in the wet season clearly due to the soil water holding capacity, while the increased number of dry days reduced the soil moisture dramatically in the dry season. This consequently leads to the reduced ET due to the insufficient soil moisture as shown in Table 4. The intensified rainfall in the wet season can raise both water yield and groundwater tables. Especially, the substantial increase in surface runoff and streamflow would intensify the floods. In the dry season with increasing number of dry days, however, the significant lower soil moisture level decreased runoff generation and groundwater recharge, which explains why the soil moisture content, monthly 7-day low flows and the annual ratio of streamflow to precipitation (RASAP) were significantly reduced (Fig. 2a, c2 and c3). This may suggest that the response of soil moisture to climate change was a critical factor causing the change in other hydrological variables such as ET, RASAP, low flows, surface runoff, streamflow and groundwater tables in the study watershed.

This case study clearly demonstrated that droughts and floods can be accelerated by shifting of rainfall and temperature patterns at the watershed scale. Our results from this study are generally consistent with other studies (Schiermeier, 2008; Piao *et al*., 2010; Porporato, 2011). However, our study addressed the connections between the changing climate and droughts and floods by elaborating the central role of soil moisture drying and shifting in rainfall intensities. In addition, this case study demonstrated a unique research methodology in addressing relative contribution of climate change to hydrology, which can be applicable to any other region where the watershed and data are comparable.

Assessing how regional climate change affects ecosystems and water resources is critical for developing appropriate strategies for public safety (Changnon & Easterling, 2000; Milly *et al*., 2008). The findings from this study have important implications to management of long-term water resource sustainability. Due to past mismanagement (i.e. deforestation, fast urbanization and other land use changes), China has greatly and frequently suffered from effects of droughts and floods. The results from this study suggest that climate change impact will further increase occurrence of floods and droughts, and place more pressures on water resource management. In addition, the extreme hydrological events (i.e. droughts and floods) caused by climate change can affect terrestrial ecosystem services and functions, and in turn, will have significant effect on social and economic well-being in China. To address those challenges, China is now conducting a large-scale campaign in reforestation (Liu *et al*., 2008) and has also recently announced an investment of 4000 billion Chinese Yuan (about 650 billion US dollars) over the next 10 years to manage and protect water resources (Chinese Central Government, 2010). Successful implementation of these large-scale initiatives must include the effect of climate change on water resources. The exacerbated floods and droughts under the climate change indicated by our study could help take precautions during the reforestation programme.

Conclusions

Using both statistical analyses of long-term observation data (i.e. climate elements and hydrological variables) and hydrological simulations, we have demonstrated that the observed soil drying, high streamflow increasing and groundwater table rising were caused by the change in precipitation patterns and air temperature as a result of climate change at the watershed scale. The intensified rainfall did not raise the soil moisture in wet season mainly due to the soil water holding capacity, but increased number of dry days reduced the soil moisture drastically in dry season, and consequently caused ET reduction due to the insufficient soil moisture. The intensified rainfall in the wet season can increase water yield, surface runoff and groundwater tables, which would augment the magnitudes of floods. In the dry season with increasing number of dry days, the significant lower soil moisture level reduced runoff generation and groundwater recharge, which led to significant reduction in soil moisture, monthly 7-day low flows and the ratio of dry season streamflow to the precipitation (RASAP). Those soil moisture and hydrological responses suggest that climate change has intensified both floods and droughts in Southern China. We also conclude that combined methodology of statistical analysis with robust hydrological modelling applied in an intact, forested watershed can be extended to any others watersheds where long-term data are available and human disturbances are negligible.

Acknowledgement

The study is supported by NSFC 30725006, 2009CB421101, NSFC40730102 and NSFG8351065005000001 and belongs to a part of CERN (Chinese Ecosystem Research Network).

References

Arabi M, Frankenberger JR, Enge BA, Arnold JG (2008) Representation of agricultural conservation practices with swat. *Hydrological Processes*, **22**, 3042–3055.

Arnold JG, Srinivasan R, Muttiah RS, Williams JR (1998) Large area hydrologic modeling and assessment - part 1: Model development. *Journal of the American Water Resources Association*, **34**, 73–89.

Arnold JG, Muttiah RS, Srinivasan R, Allen PM (2000) Regional estimation of base flow and groundwater recharge in the upper mississippi river basin. *Journal of Hydrology*, **227**, 21–40.

Buol SW, Southard RJ, Graham RC, McDaniel PA (2003) *Soil Genesis and Classification* (5th edn). Iowa State Press, Iowa, USA, pp. 339–347.

Changnon SA, Easterling DR (2000) Disaster management – U.S. policies pertaining to weather and climate extremes. *Science*, **289**, 2053–2055.

Chinese Central Government (2010) *On the decision of speeding up the development of water resources management*. Available at: http://www.ce.cn/xwzx/gnsz/szyw/201101/30/t20110130_22183115.shtml (accessed 31 December 2010).

Dirmeyer PA (2000) Using a global soil wetness dataset to improve seasonal climate simulation. *Journal of Climate*, **13**, 2900–2922.

Easterling DR, Evans JL, Groisman PY, Karl TR, Kunkel KE, Ambenje P (2000a) Observed variability and trends in extreme climate events: a brief review. *Bulletin of the American Meteorological Society*, **81**, 417–425.

Easterling DR, Meehl GA, Parmesan C, Changnon SA, Karl TR, Mearns LO (2000b) Climate extremes: observations, modeling, and impacts. *Science*, **289**, 2068–2074.

Eckhardt K, Ulbrich U (2003) Potential impacts of climate change on groundwater recharge and streamflow in a central european low mountain range. *Journal of Hydrology*, **284**, 244–252.

Ficklin DL, Luo YZ, Luedeling E, Zhang MH (2009) Climate change sensitivity assessment of a highly agricultural watershed using swat. *Journal of Hydrology*, **374**, 16–29.

Fischer EM, Seneviratne SI, Vidale PL, Luthi D, Schar C (2007) Soil moisture - atmosphere interactions during the 2003 european summer heat wave. *Journal of Climate*, **20**, 5081–5099.

Gao Q, Zhao P, Zeng X, Cai X, Shen W (2002) A model of stomatal conductance to quantify the relationship between leaf transpiration, microclimate and soil water stress. *Plant Cell and Environment*, **25**, 1373–1381.

14Green CH, van Griensven A (2008) Autocalibration in hydrologic modeling: using swat2005 in small-scale watersheds. *Environmental Modelling & Software*, **23**, 422–434.

Guangdong Soil Survey Office (GSSO) (1993) *Guangdong Soil*. Science Press, Beijing.

Hassler GL, Brunner E (1945) Measurement of capillary pressures in small core samples. *Transactions of the American Institute of Mining and Metallurgy Engineers*, **160**, 23–32.

Hong SY, Kalnay E (2000) Role of sea surface temperature and soil-moisture feedback in the 1998 oklahoma-texas drought. *Nature*, **408**, 842–844.

IPCC (2007) Climate change 2007: The physical science basis. Contribution of working group i to the fourth assessment report of the intergovernmental panel on climate change. IPCC, Cambridge, United Kingdom and New York, NY, USA.

Jackson RB, Carpenter SR, Dahm CN *et al*. (2001) Water in a changing world. *Ecological Applications*, **11**, 1027–1045.

Karl TR, Knight RW (1998) Secular trends of precipitation amount, frequency, and intensity in the united states. *Bulletin of the American Meteorological Society*, **79**, 231–241.

Koster RD, Dirmeyer PA, Guo ZC *et al*. (2004) Regions of strong coupling between soil moisture and precipitation. *Science*, **305**, 1138–1140.

Koster RD, Suarez MJ (2003) Impact of land surface initialization on seasonal precipitation and temperature prediction. *Journal of Hydrometeorology*, **4**, 408–423.

Liu JG, Li SX, Ouyang ZY, Tam C, Chen XD (2008) Ecological and socioeconomic effects of china's policies for ecosystem services. *Proceedings of the National Academy of Sciences of the United States of America*, **105**, 9477–9482.

Luo Y, Liu S, Fu SL, Liu JS, Wang GQ, Zhou GY (2008) Trends of precipitation in beijiang river basin, guangdong province, china. *Hydrological Processes*, **22**, 2377–2386.

Mason SJ, Waylen PR, Mimmack GM, Rajaratnam B, Harrison JM (1999) Changes in extreme rainfall events in south africa. *Climatic Change*, **41**, 249–257.

Medlyn BE, Barton CVM, Broadmeadow MSJ *et al*. (2001) Stomatal conductance of forest species after long-term exposure to elevated co2 concentration: a synthesis. *New Phytologist*, **149**, 247–264.

Milly PCD, Betancourt J, Falkenmark M *et al*. (2008) Climate change - stationarity is dead: whither water management? *Science*, **319**, 573–574.

Muleta MK, Nicklow JW (2005) Sensitivity and uncertainty analysis coupled with automatic calibration for a distributed watershed model. *Journal of Hydrology*, **306**, 127–145.

Neitsch SL, Arnold JG, Kiniry JR, Williams JR, King KW (2005) *Soil and water assessment tool theoretical documentation*. Grassland, soil and research service, Temple, TX.

New M, Todd M, Hulme M, Jones P (2001) Precipitation measurements and trends in the twentieth century. *International Journal of Climatology*, **21**, 1899–1922.

Piao SL, Ciais P, Huang Y *et al*. (2010) The impacts of climate change on water resources and agriculture in china. *Nature*, **467**, 43–51.

Piao SL, Yin L, Wang XH *et al*. (2009) Summer soil moisture regulated by precipitation frequency in china. *Environmental Research Letters*, **4**, doi: 10.1088/1748-9326/4/4/044012.

Porporato A (2011) Hydrology: melting to the max. *Nature*, **470**, 439.

Qiu J (2010) China drought highlights future climate threats. *Nature*, **465**, 142–143.

Robock A, Li HB (2006) Solar dimming and CO_2 effects on soil moisture trends. *Geophysical Research Letters*, **33**, doi: 10.1029/2006GL027585.

Santhi C, Arnold JG, Williams JR, Dugas WA, Srinivasan R, Hauck LM (2001) Validation of the swat model on a large river basin with point and nonpoint sources. *Journal of the American Water Resources Association*, **37**, 1169–1188.

Saxe H, Ellsworth DS, Heath J (1998) Tree and forest functioning in an enriched co2 atmosphere. *New Phytologist*, **139**, 395–436.

Schiermeier Q (2008) Water: a long dry summer. *Nature*, **452**, 270–273.

Seneviratne SI, Luthi D, Litschi M, Schar C (2006) Land-atmosphere coupling and climate change in europe. *Nature*, **443**, 205–209.

Shukla J, Mintz Y (1982) Influence of land-surfacce evapo-transpiration on the earth's climate. *Science*, **215**, 1498–1501.

Tang XL, Wang YP, Zhou GY (2011) Different patterns of ecosystem carbon accumulation between a young and an old-growth subtropical forest in southern china. *Plant Ecology*, **212**, 1385–1395, doi: 10.1007/s11258-011-9914-2.

van Griensven A, Meixner T, Grunwald S, Bishop T, Diluzio A, Srinivasan R (2006) A global sensitivity analysis tool for the parameters of multi-variable catchment models. *Journal of Hydrology*, **324**, 10–23.

Wand SJE, Midgley GF, Jones MH, Curtis PS (1999) Responses of wild c4 and c3 grass (poaceae) species to elevated atmospheric co2 concentration: a meta-analytic test of current theories and perceptions. *Global Change Biology*, **5**, 723–741.

Wei XH, Zhang M (2010a) Research methods for assessing the impacts of forest disturbance on hydrology at large-scale watersheds. In: *Landscape Ecology and Forest Management: Challenges and Solutions in a Changing Globe* (eds Li C, Lafortezza R, Chen J), pp. 119–147. Springer, Jointly with Higher Education Press, New York.

Wei XH, Zhang MF (2010b) Quantifying streamflow change caused by forest disturbance at a large spatial scale: a single watershed study. *Water Resources Research*, **46**, doi: 10.1029/2010WR009250.

Winchell M, Srinivasan R, Di Luzio M, Arnold JG (2009) *Arcswat 2.3.4 interface for swat2005*. Grassland, soil and research service, Temple, TX.

Wolock DM, McCabe GJ (1999) Estimates of runoff using water-balance and atmospheric general circulation models. *Journal of the American Water Resources Association*, **35**, 1341–1350.

Wu Y, Liu S, Abdul-Aziz OI (2011) Hydrological effects of the increased CO_2 and climate change in the upper mississippi river basin using a modified swat. *Climatic Change*, doi: 10.1007/s10584-011-0087-8 (in press).

Yan JH, Zhou GY, Chen ZY (2001a) Potential evapotranspiration of artificial pinus forest in mount dinghu and the comparison of calculation methods. *Chinese Journal of Ecology*, **20**, 5–8. (Chinese with English abstract).

Yan JH, Zhou GY, Huang ZL (2001b) Evapotranspiration of the monsoon evergreen broad-leaf forest in dinghushan, guangdong province. *Scientia Silvae Sinicae*, **37**, 37–45. (Chinese with English abstract).

Yan JH, Zhou GY, Zhang DQ, Wang X (2003) Spatial and temporal variations of some hydrological factors in a climax forest ecosystem in the Dinghushan region. *Acta Ecollogica Sinica*, **23**, 2359–2366. (Chinese with English abstract).

Zhang M, Ren Q, Wei X, Wang J, Yang X, Jiang Z (2011) Climate change, glacier melting and streamflow in niyang river basin, southeast tibet, china. *Ecohydrology*, **4**, 288–298.

Zhou GY, Guan LL, Wei XH *et al*. (2007) Litterfall production along successional and altitudinal gradients of subtropical monsoon evergreen broadleaved forests in guangdong, china. *Plant Ecology*, **188**, 77–89.

Zhou GY, Wei XH, Luo Y *et al*. (2010) Forest recovery and river discharge at the regional scale of guangdong province, china. *Water Resources Research*, **46**, doi: 10.1029/2009WR008829.